

Molecular-to-Macroscopic Interfacial Remodeling of Oil-Water Systems under DC Electric Fields: Mechanisms and Applications in Enhanced Recovery and Wastewater Treatment

Qiang Li^{1,2}, Zhengfu Ning^{1,2*}, Jun Li^{1,2}, Kangbo Zhao^{1,2}, Xiqian Zheng^{1,2}, Yuheng Yang^{1,2}, Zejiang Jia³

1 National Key Laboratory of Petroleum Resources and Engineering, China University of Petroleum (Beijing), 102249, Beijing, China

2 College of Petroleum Engineering, China University of Petroleum (Beijing), Beijing 102249, China

3 Oil production Technology Research Institute, Dagang Oilfield Branch Company, PetroChina, Dagang, Tianjin, China

(Corresponding Author: ningzhengfu313@163.com)

ABSTRACT

This study investigates how DC electric fields (0-15 V) regulate interfacial properties and compositional evolution in crude oil – water systems. By integrating IFT and interfacial viscosity measurements with aqueous chemical analysis, SARA fractionation, GC, and FTIR, we reveal correlations between aqueous electrochemistry and molecular restructuring of crude oil. Electrolysis at the cathode increased aqueous pH to 12.97, promoting ionization of native acids and in-situ formation of carboxylates; correspondingly, IFT dropped from 12.63 to 0.08 mN·m⁻¹. Interfacial viscosity decreased sharply with voltage, while SARA and molecular analyses showed depletion of asphaltenes, ~eightfold growth of polar resins, ~9.6% rise in branched alkanes, and ~32% increase in the CH₃/CH₂ ratio. These coupled aqueous–oil transformations explain the collapse of interfacial film strength under DC electrolysis and suggest a dual mechanism: aqueous alkalinization activates the interface, while electrochemically induced molecular restructuring weakens it. The findings directly inform electrochemical EOR and demulsification strategies.

Keywords: DC electric field; Interfacial tension; Molecular reconstruction; Carboxylation; Electrorheological synergy; enhanced oil recovery

NONMENCLATURE

Abbreviations

SARA	Saturates, Aromatics, Resins, Asphaltenes
GC	Gas Chromatography
FTIR	Fourier Transform infrared spectroscopy
DC	Direct Current
EOR	Enhanced Oil Recovery
IFT	Interfacial Tension

1. INTRODUCTION

Petroleum resources are essential to modern society as energy sources and chemical feedstocks, directly influencing energy security and sustainable development. However, conventional recovery methods leave large amounts of oil unrecovered, making EOR a persistent challenge[1][2]. Meanwhile, treating oily wastewater across the petroleum lifecycle poses major technical and economic pressures. Oil–water interfacial properties—particularly IFT and interfacial viscosity—govern crude oil displacement in porous media and droplet coalescence in wastewater[3][4][5][6], with film strength and dynamic shear response being especially critical[7][8]. Thus, techniques to modulate these interfacial properties are key to improving hydrocarbon utilization.

Currently, regulation relies mainly on chemical methods[3][4], which, though partly effective, involve high costs, environmental risks, and downstream complications[9]. In contrast, physical approaches—especially electric fields—offer advantages such as environmental compatibility, rapid response, controllable energy use, and ease of automation. Electric fields have long been applied in electrostatic coalescence for dehydration, and concepts for EOR exist[10][11][12]. Yet most research emphasizes electric-field-induced IFT reduction via charge redistribution, electrowetting, or electrochemistry, while the direct effects of DC fields on interfacial rheology—particularly viscosity and shear dependence—remain poorly understood[13].

Critical gaps persist. The coupled variation of IFT and viscosity under DC fields is unclear, and electrochemical reactions alter both oil and aqueous phases[14][15], but their correlation with interfacial changes is underexplored. Moreover, a direct, quantitative research chain linking DC-field modulation of interfacial

properties to applications in EOR and wastewater treatment is incomplete, limiting technological development.

To address these gaps, this study applies a multiscale experimental approach to examine electrolysis effects of DC fields on oil–water interfaces and assess application potential. Objectives include systematically measuring DC field impacts on IFT and interfacial viscosity; investigating field-induced changes in crude oil composition via GC and SARA analysis; and measuring alterations in aqueous phase pH and major ion concentrations post-treatment. This work elucidates the physicochemical basis of DC-field modulation at the oil–water interface and provides a foundation for efficient, environmentally friendly EOR and wastewater treatment technologies.

2. EXPERIMENTAL SECTION

2.1 Experimental materials

The crude oil used in this study was degassed oil from the Mahu area of the Junggar Basin, Xinjiang Uygur Autonomous Region, China. It underwent dehydration, filtration, and other treatments to remove impurities. Compositional analysis according to the standard method yielded the following: asphaltenes (3.98 wt.%), saturates (84.94 wt.%), aromatics (9.66 wt.%), and resins (1.42 wt.%). The brine employed was synthetic formation water, prepared using analytical-grade reagents purchased from Beijing Chemical Works, China: sodium chloride (NaCl, 99.5%), calcium chloride (CaCl₂, 99.5%), sodium bicarbonate (NaHCO₃, 99.5%), sodium sulfate (Na₂SO₄, 99.5%), and magnesium chloride hexahydrate (MgCl₂·6H₂O, 99.5%). Deionized water was prepared using an ultrapure water system. The ionic composition of the formation water is detailed below (unit: mg/L):

Table 1. Formation water ion composition

Na ⁺	Ca ²⁺	Mg ²⁺	Cl ⁻	SO ₄ ²⁻	HCO ₃ ⁻
18394.90	71.74	187.16	25873.47	58.60	5115.12

To prevent redox reactions at the electrodes due to the applied voltage, platinum electrodes were used. A Longwei TPR-3005D DC power supply, providing stable voltage with a precision of 0.1 V, was employed. Gas sampling bags (2L capacity, ≤6kPa fill pressure) constructed of aluminum-plastic composite film were purchased from Dalian Haide Technology Co., Ltd. Standard laboratory apparatus included a three-necked flask, iron stand clamp, thermometer, condenser unit, and rubber tubing.

2.2 Experimental methods

An experimental setup was constructed using the described materials. Prepared brine solutions and treated crude oil samples were used. First, brine and crude oil were added to the three-necked flask in a 1:1 volume ratio. The condenser unit was activated and connected to a gas collection system at the outlet. The system temperature was monitored and maintained at 25°C. Second, the DC power supply was connected, and electrolysis was conducted for 12 hours at applied voltages of 5V, 10V, and 15V. Upon completion, the power supply was switched off, and the reaction vessel was allowed to cool to room temperature before stopping the condenser water flow. The reacted mixture was then transferred to a separatory funnel, sealed, and allowed to settle undisturbed for at least 24 hours to achieve a stable oil-water interface. Finally, the reacted aqueous phase (bottom layer) and oil phase (top layer) were carefully sampled from the funnel, sealed, protected from light, and stored for subsequent analysis.

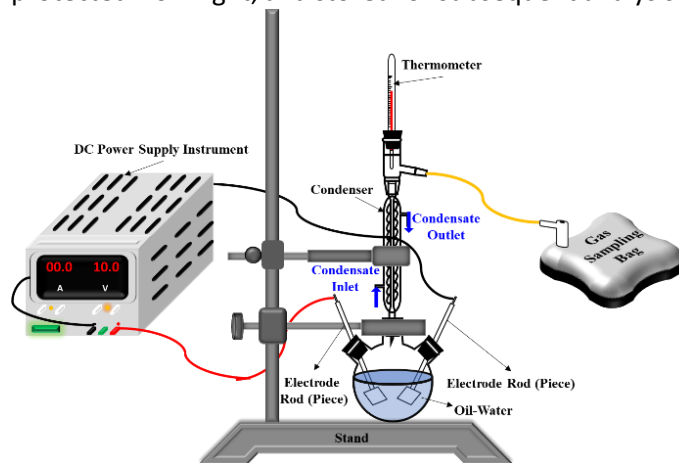


Fig. 1 Experimental setup diagram

IFT Measurement: IFT was measured using a Kono TX500C spinning drop tensiometer (USA) at 25°C and a rotational speed of 6000 rpm. Centrifuge tubes were meticulously cleaned with acetone prior to each measurement to ensure no contamination. Each sample was measured in triplicate, and the average value was reported to minimize error.

Interfacial Rheology Measurement: Interfacial viscosity was determined using a Physica MCR 301 rheometer (Austria) equipped with a Du Noüy ring geometry at 25°C. Shear rates ranged from 1 to 100 s⁻¹. The measuring geometry was calibrated prior to experiments. The aqueous phase was placed in the measuring cup, and the ring geometry was positioned precisely at the interface. Subsequently, 30 mL of crude oil was carefully layered on top. The cup was sealed and the interface was allowed to equilibrate for at least 30 minutes before commencing measurements.

Aqueous Phase pH and Ion Concentration Measurement: pH was measured using a PHSJ-3F pH meter (China) with a precision of 0.01 units at 25°C. The instrument was calibrated using standard buffer solutions before each measurement. Each sample (20 mL of aqueous phase) was measured in triplicate, and the average value was reported. Ion concentrations were analyzed using an ICP-OES OPTIMA 7300 spectrometer (USA). Samples were diluted with deionized water to concentrations between 1 and 10 mg/L prior to analysis, with deionized water used as a blank control.

Crude Oil Compositional Analysis: The four-component analysis of crude oil was conducted in accordance with the current industry standard for the determination of petroleum asphalt four components issued by the People's Republic of China (NB/SH/T 0509-2010).

Hydrocarbon Analysis: Hydrocarbon distribution was analyzed using a Thermo Fisher Trace 1300 Gas Chromatograph (USA). The injector temperature was set to 450°C to ensure complete vaporization of the oil sample, guaranteeing result accuracy.

FTIR Spectroscopy: FTIR spectra were acquired using a VERTEX 80v spectrometer (Germany) with a resolution of 4 cm⁻¹ over the range 400-4000 cm⁻¹. Prior to sample analysis, a background scan was performed using a clean potassium bromide (KBr) disk. Oil samples were analyzed using the thin-film method: a small droplet of oil was deposited onto the KBr disk using a micro-syringe and scanned immediately. The disk was thoroughly cleaned with anhydrous ethanol after each measurement.

3. RESULTS

3.1 Electro-Responsive Manipulation of Interfacial Properties

Application of DC voltage produced rapid, voltage-dependent reductions in static interfacial tension (Fig.2 (a)): the baseline IFT of 12.63 mN·m⁻¹ fell to 1.82 mN·m⁻¹ at 5V, 0.68 mN·m⁻¹ at 10V and reached 0.08 mN·m⁻¹ at 15V. The largest incremental change occurs between 0 V and 5V, with diminishing marginal decrease at higher voltages; this suggests that the primary interfacial activation occurs once a threshold of interfacial surfactant activity and charge rearrangement is achieved, while higher voltages amplify but do not linearly scale the effect.

Interfacial rheology measurements reveal a pronounced electro-rheological response coupled to shear (Fig.2 (b)): all conditions show shear-thinning, but increasing DC voltage systematically lowers the absolute

interfacial viscosity across the low-to-moderate shear regime. At a representative shear rate of 10s⁻¹, interfacial viscosity falls from 0.327Pa·s·m to 0.0268Pa·s·m, an approximate 91.8% reduction. A critical shear rate (about 31.6 s⁻¹) marks the onset of a partial viscosity rebound at the highest voltage, which we interpret as rapid polarization and restructuring of the residual interfacial network under combined strong electric and mechanical forcing; despite this rebound, the absolute viscosity at 15V remains the lowest across the tested shear range. Collectively, the data demonstrate that DC electrolysis both weakens the interfacial film and modifies its dynamic response to shear, which has immediate consequences for displacement and coalescence processes.

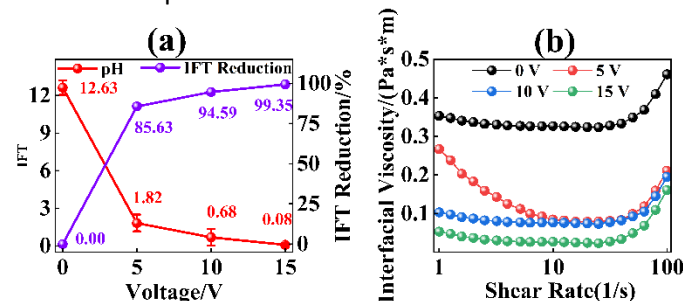


Fig. 2 (a) IFT versus Voltage Variation Diagram
(b) Interface viscosity versus voltage variation graph

3.2 Electrochemically-Driven Alterations in Aqueous Phase Chemistry

Electrochemical treatment induced significant voltage-dependent alterations in the ionic distribution and pH of the aqueous solution. As the applied voltage increased, the pH rose progressively from an initial value of 8.46 to 12.97 (Fig.3 (a)). This pronounced alkalinization is attributed to enhanced hydrolysis reactions at the cathode, leading to the continuous generation of OH⁻ ions. Such highly alkaline solutions readily interact with acidic components present in crude oil, contributing significantly to the observed reduction in interfacial tension.

A noteworthy observation concerns sodium ion (Na⁺) concentration (Fig.3(b)). While the initial diluted solution had a Na⁺ concentration of 3.68mg/L, post-treatment measurements revealed an increase rather than a decrease. This phenomenon is directly linked to electromigration mechanisms: under the influence of the electric field, Na⁺ ions migrate directionally towards the cathode, resulting in localized enrichment. As the aqueous phase was sampled as a bulk solution, the measured concentration reflects a dynamic equilibrium between migration and diffusion processes. Although the elevated OH⁻ concentration at higher voltages might

promote precipitation of some cations (e.g., Ca^{2+} and Mg^{2+}), Na^+ ions, due to their higher solubility, maintained a measurable increase.

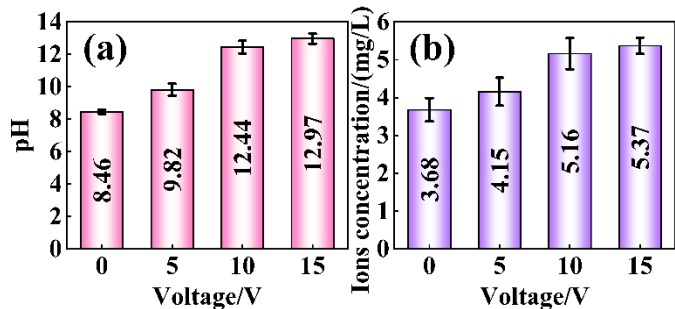


Fig. 3 (a) PH versus Voltage Variation Diagram

(b) Ionic concentration versus voltage variation graph

3.3 DC Electric Field-Induced Molecular Restructuring of Crude Oil Components

The SARA fractionation results showed pronounced compositional shifts under DC electric field treatment (Fig.4 (a)). Asphaltene content decreased by about 40% compared with the untreated sample, while the resin fraction rose sharply from 1.42% to 11.25% at 15V — nearly a tenfold increase. Saturates and aromatics exhibited only slight overall reductions. The decrease in asphaltenes, coupled with the increase in resins, contributed directly to the substantial declines in both crude oil shear viscosity and interfacial properties.

Gas chromatography further revealed specific alterations in hydrocarbon composition. Cycloalkanes remained largely unaffected, fluctuating only slightly between 7.14% and 7.22%. n-alkanes decreased by 4–5%, suggesting cracking or structural transformation of straight chains. Branched alkanes increased from 28.05% at 0V to 30.75% at 5V, remaining above 30% at higher voltages, indicating enhanced isomerization. Benzene-ring compounds rose from 5.44% to 7.60% at 15V, pointing to voltage-induced aromatization (Fig.4(b)). Together, these findings demonstrate that DC treatment reconstructs crude oil composition primarily through isomerization and aromatization pathways.

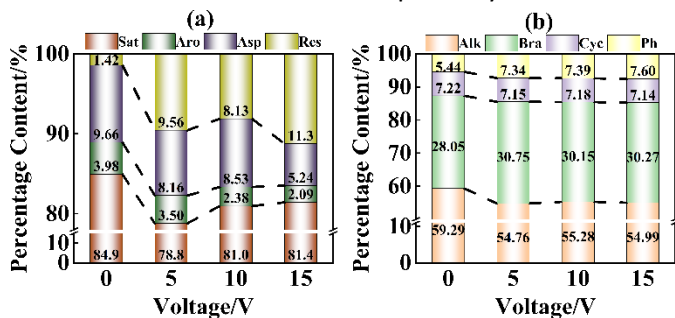


Fig. 4 (a) SARA analysis chart

(b) Gas Chromatography Analysis Chart

FTIR analysis of functional group ratios confirmed extensive molecular restructuring (Fig.5 (a-1)). The carboxylic acid/carboxylate ratio dropped by 58%, reflecting alkaline-promoted ionization and carboxylate formation. The aldehyde/carboxylic acid ratio fell by 34%, with minima at 5V and 15V, indicating voltage-dependent oxidation kinetics. The CH_2/CH_3 ratio rose steadily by 32% to exceed unity at 15V, evidencing increased chain branching via radical-mediated methyl substitution. Meanwhile, the mono-/di-substituted benzene ratio (S-B/D-B) declined sharply, stabilizing thereafter, consistent with substitution pattern reorganization toward more stable di-substituted structures (Fig.5 (b1~4)). These molecular-level transformations (encompassing carboxylate generation, oxidation, branching, and aromatic substitution shifts) clarify the electrochemical mechanisms underpinning the observed interfacial property changes and support targeted electrochemical modification strategies for crude oil.

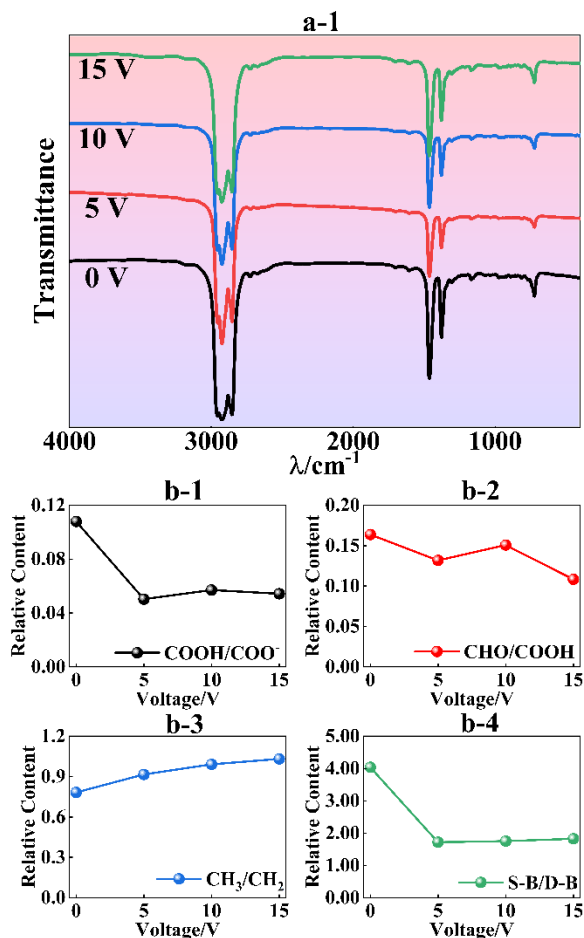


Fig. 5 (a-1) FTIR spectra corresponding to different voltages

(b1~4) Changes in relative content of different functional groups

4. DISCUSSION

DC electric fields demonstrably reconstruct the interfacial properties of crude oil-water systems, revealing the molecular mechanism underpinning electrochemical EOR. Cathodic alkalization is the primary, rapid driver of interfacial activation: OH⁻ production shifts equilibria, converting indigenous petroleum acids into carboxylates that preferentially partition to and stabilize at the interface, thereby reducing IFT. Simultaneously, electrochemical oxidation and radical chemistry at or near the anode and within the bulk oil produce structural changes — cracking of long n-alkanes, isomerization to branched forms, and generation of more polar fragments — that lower the oil's propensity to form strong asphaltene networks at the interface. The result is a dual-path synergy: aqueous activation supplies amphiphiles while oil restructuring reduces the reservoir of film-forming macromolecules. The observed partial viscosity rebound at high shear and high voltage points to dynamic polarization and reassembly kinetics of remaining interfacial species: when mechanical forcing is sufficient, polarized fragments and residual asphaltene aggregates can transiently reorient and re-aggregate, increasing resistance; however, because the pool of film-forming material is substantially reduced, the rebound does not restore baseline strength. Practically, this rheo-electrochemical coupling suggests that DC treatment may be most effective when combined with flow regimes that exploit reduced low-shear film strength (e.g., enhanced mobilization during low-rate flooding) and when managed to avoid shear conditions that favour temporary reformation. Notably, the anomalous rebound in interfacial viscosity observed under high shear rates (>31.6 s⁻¹) at high voltage (15V) suggests that polarization effects may accelerate dynamic reconstruction of the interfacial film. Crucially, however, the absolute viscosity remains lower than the baseline value, demonstrating the applicability of strong electric fields even under the high-shear conditions typical of deep reservoirs. In summary, the electric field achieves efficient interfacial property optimization through the synergistic regulation of aqueous phase alkalinity, ion migration, and polar transformation of crude oil molecules, providing a solid theoretical foundation for electrochemical EOR.

5. CONCLUSIONS

This study systematically investigated the influence of DC electric fields on the interfacial properties and compositional evolution of crude oil-water systems,

revealing the intrinsic mechanism of electrochemically driven interfacial reconstruction. The main conclusions are as follows:

(1) DC electric fields efficiently weaken interfacial barriers through dual actions. The applied voltage continuously elevates the aqueous phase pH into the strongly alkaline range via cathodic hydrolysis, promoting the ionization of carboxylic acids within the crude oil to generate in-situ surfactants. This process drives the interfacial tension down to 0.08mN/m at 15V. Concurrently, interfacial viscosity is significantly reduced, primarily due to the structural weakening of the interfacial film caused by a 40% decrease in asphaltene content combined with a nearly tenfold surge in polar non-hydrocarbon components.

(2) Furthermore, long-lasting effects are governed by the molecular restructuring of crude oil components. The electric field triggers directed transformations in hydrocarbon structures, evidenced by a 9.6% increase in branched alkanes resulting from the cracking/isomerization of n-alkanes. FTIR analysis further corroborates a branching trend, showing a 32% rise in the methyl-to-methylene ratio, while a sharp 55% decline in the mono-to-disubstituted benzene ratio reveals substantial reorganization of aromatic ring substituents. This molecular-level restructuring provides a persistent driving force for optimizing interfacial properties.

(3) Critically, the electrochemical-rheological synergy enhances operational adaptability. The anomalous rebound in interfacial viscosity observed under high shear rates at high voltage (15V) indicates accelerated dynamic interfacial reorganization induced by polarization effects. Crucially, the absolute viscosity remains at its lowest level, confirming the significant technical advantage of strong electric fields even under the high-shear conditions prevalent in deep reservoirs. This electrochemical-rheological synergistic mechanism establishes a novel framework for the targeted design of efficient oil recovery technologies.

ACKNOWLEDGEMENT

This work was supported by The National Natural Science Foundation of China (No. 51974330).

REFERENCE

- [1] Alvarado V.; Manrique E. Enhanced Oil Recovery: An Update Review. *Energies* 2010;3:1529-1575.
- [2] Liu ZX, Liang Y, Wang Q, et al. Status and progress of worldwide EOR field applications. *J Pet Sci Eng* 2020;193:107449.

- [3] Yousefrouz A, Shabani MH, Jafari A et al. Interfacial tension reduction and viscosity control by chemically grafted polymeric surfactant for enhanced oil recovery. *Sci Rep* 2025;15:11607.
- [4] Chen X, Li YQ, Liu ZY, et al. Experimental investigation on the enhanced oil recovery efficiency of polymeric surfactant: Matching relationship with core and emulsification ability. *Pet Sci* 2023;20(1):619-635.
- [5] Reis PKP, Carvalho MS. Pore-scale compositional modeling of gas-condensate flow: Effects of interfacial tension and flow velocity on relative permeability. *J Pet Sci Eng* 2021;202:108454.
- [6] Shabani MH, Jafari A, Manteghian M, et al. Green synthesis of zinc oxide nanoparticles using *Enterobacter cloacae* microorganism and their application in enhanced oil recovery. *Sci Rep* 2024;14:29409.
- [7] Jiang H, Liu XY, Liang CH, et al. Effect of asphaltenes structure on interfacial properties: A dissipative particle dynamics study. *Colloids Surf A* 2023;673:131849.
- [8] Ganeeva YM, Barskaya EE, Okhotnikova ES, et al. Characteristics of Asphaltene Fractions Responsible for the Formation of Stable Water-Oil Emulsions. *Chem Technol Fuels Oils* 2024;59:1162–1168.
- [9] Solcova O, Dlaskova M, Kastanek F. Challenges and Advances in Tertiary Waste Water Treatment for Municipal Treatment Plants. *Processes* 2024;12(10):2084.
- [10] Bai X, Liu YT, Kang Y. Demulsification performance of oil-in-water emulsions utilizing bidirectional pulse electric field and fiber media. *Sep Purif Technol* 2025;367:132923.
- [11] Li MF, Yang DH, Zhong HX, et al. Enhancing dewatering and desalination of crude oil: A comprehensive study on energy-efficient separation technology driven by electric–magnetic coupling field. *Sep Purif Technol* 2025;361:131501.
- [12] Lang XJ, Bai X, Feng JY, et al. Synergistic demulsification of oil-in-water emulsion using bidirectional pulse electric field and fiber coalescence. *J Water Process Eng* 2024;66:105967.
- [13] Singh N, Narsimhan V. Effect of Droplet Viscosity Ratio and Surfactant Adsorption on the Coalescence of Droplets with Interfacial Viscosity. *Fluids* 2024;9(2):48.
- [14] Li Q, Ning ZF, Zheng XQ, et al. Chemical properties and interfacial behavior of fluids during enhanced oil recovery under direct current electric fields. *Colloids Surf A* 2025;725(1):137591.
- [15] Li Q, Ning ZF, Li J, et al. Laboratory study on the transformation of oil-water interface properties under direct current electric field. *Geoenergy Sci Eng* 2024;239:212953.